Hindawi
Advances in Materials Science and Engineering
Volume 2019, Article ID 5819805, 8 pages
https://doi.org/10.1155/2019/5819805

Research Article

Antibacterial Activity of Visible Light-Activated TiO_2 Thin Films with Low Level of Fe Doping

Dan Meng, Xiuhua Liu, Yun Xie, Yang Du, Yong Yang, and Chao Xiao

Institute of Nuclear Physics and Chemistry, China Academy of Engineering Physics, Mianyang 621900, China

Correspondence should be addressed to Chao Xiao; xiaochao@caep.cn

Received 5 July 2019; Revised 16 September 2019; Accepted 25 September 2019; Published 25 November 2019

Academic Editor: Saliha Ilican

Development of effective antibacterial visible light-activated photocatalytic materials in industries including wastewater treatment and food industry has attracted increasing attention. In this work, Fe-doped TiO_2 thin films with different doping levels on a glass substrate were prepared by the sol-gel dip-coating method. The as-prepared films were characterized by Raman spectroscopy, X-ray diffraction (XRD), X-ray photoelectron spectroscopy (XPS), and atomic force microscope (AFM). Raman spectroscopy and XRD results show the crystalline phase of titanium dioxide was anatase, and the range of the crystal size for the films was 19.24–22.24 nm. XPS results indicate that iron was in the form of Fe^{3+} in Fe-doped TiO_2 films. Regarding the antibacterial properties of TiO_2 films, the order of antibacterial activity of TiO_2 films was 0.1 at% Fe > 0.5 at% Fe > 1.0 at% TiO_2 > bare TiO_2 > 2.0 at% Fe > 3.45 at% Fe. 0.1 at% of Fe is the optimum dopant ratio related to antibacterial activity. 0.1 at% Fe-doped TiO_2 film is highly efficient in inactivating E. coli under 3 h of visible light irradiation, and it remains efficient even in real dye waste water.

1. Introduction

Visible and solar light-active semiconductor photocatalysis has been greatly documented for antibacterial application in food industry, environmental, hospital, and wastewater treatment [1–8]. Among these semiconductor materials, TiO_2 is probably the most widely studied one owing to a great deal of advantages, i.e., low cost, ready availability, high chemical stability, nontoxicity, environmental friendliness, etc. [9–11].

As early as in 1999, Fujishima et al. [12] reported that TiO_2 can kill bacteria on its surface. Since then, there has been increasing attention in the antibacterial property of TiO_2. However, anatase TiO_2 has a relatively large band gap of 3.2 eV and can only be activated under the irradiation of UV light ($\lambda \leq 387$ nm), which limits its utilization in visible and solar irradiation [13]. Therefore, in order to extend the spectral response to visible light region, efforts to combine TiO_2 with other elements such as metal deposition [11, 14–17], nonmetal doping [18–21], and metal and nonmetal codoping [22, 23] have been carried out. Doping TiO_2 with transition metals such as Fe [11, 24], Cr [25], Cu [26, 27], and Zn [28] is a simple and effective method. More recently, antibacterial properties of TiO_2 with various morphologies such as graphene nanosheet doped TiO_2 [29], titania nanotubes [6], and Fe-Ag/TiO_2 bimetallic nanowires [30] were reported.

Fe has attracted extensive attention because its octahedral trivalent radius (0.079 nm) is similar to that of titanium's octahedral tetrahedron (0.075 nm) [10]. Introduction of iron in the titania crystal lattice can form a new energy level between the valence band and conduction band, resulting in an extension of light absorption of TiO_2 into the visible region [4, 31, 32]. The antibacterial property of Fe-doped TiO_2 under UV irradiation has been widely studied [10, 33–37], which shows the Fe-doped TiO_2 has excellent antibacterial properties against *E. coli* and *S. aureus*, some of which can be as high as 100% [10, 35]. Antibacterial activity of Fe^{3+}- doped TiO_2 nanoparticles was studied by Boonyod S et al. [38], which reported that 0.5 mol % Fe^{3+}/TiO_2 can destroy *E. coli* after 20 min with UV irradiation. More recently, AL-Jawad et al. [11] found that the antibacterial efficiency of 6% Fe-doped TiO_2 thin films against *E. coli* and *S. aureus* can both reach 100% under UV light. However, these reports mostly tested antibacterial properties of Fe-doped TiO_2 under UV irradiation, rarely under visible light irradiation. Arellano et al. [34] reported the antimicrobial activity under visible light irradiation of TiO_2 thin films with 3 wt% and 5 wt% of Fe on the glass substrate by the spin-coating method. They found that doping TiO_2 film with 5 wt % of Fe treated at 800°C can eliminate the bacteria completely after 60 min.

In order to explore the effect of iron content on the antibacterial properties of TiO_2 thin film visible light irradiation, TiO_2 films with different iron contents by the sol-gel dip-coating method on the glass substrate were prepared in our work. These series of Fe-doped TiO_2 thin films were characterized by Raman spectroscopy, XRD, XPS, and AFM. The optimum dopant ratio is 0.1 at%, with the best antibacterial activity even in real dye waste water.

2. Experimental

2.1. Preparation of TiO_2 Thin Films. Fe-doped TiO_2 thin films were prepared by the sol-gel dip-coating method. For the preparation of sol, 10 ml of $Ti(OBu)_4$ as precursor solution was added to 26 ml of ethanol under stirring at room temperature, and continued stirring vigorously for 0.5 h. After stirring, a mixed solution containing 20 ml of ethanol, 1.05 ml of concentrated hydrochloric acid, some water and different amounts of $FeCl_3{\cdot}6H_2O$ was added dropwise to the above solution under stirring followed by a 2-hour hydrolysis period and 24-hour ageing period, resulting in the Fe-doped sol. The atomic ratios of Fe to Ti were 0, 0.1, 0.5, 1.0, 2.0, and 3.45 at%.

For the preparation of the films, ordinary glass slides were used as the supporting substrate (75.0 mm × 25.0 mm × 1.2 mm) after soaked in acid pail for 24 h and ultrasonic cleaning with ethanol for 3 times. The cleaned and dried glass slides were dipped in the above sol for 1.5 min and then withdrew at 1.94 $mm{\cdot}s^{-1}$. After the gel films came to dryness at room temperature, they were calcined in muffle furnace at 450°C for 2 h in air. For the preparation of multilayered films, the gel films were left in the furnace at 450°C for 10 min after each coating cycle and finally calcined at 450°C for 2 h. In our experiments, the coating was repeated from one to five times, and the thickness of the TiO_2 films is 150 nm–370 nm, as shown in supporting information (Figure S1). Five-layered films were used for characterization and antibacterial test.

2.2. Characterization. Raman spectra were recorded with a confocal Raman spectroscopy with the Raman shift ranging from 0 to 1000 cm^{-1} (Jobin Yvon, HR 800). The crystal phase and crystal size of the obtained TiO_2 films were investigated by X-ray diffraction (Philips, MPD-MPDXPERT) with the diffraction angles scanning from $2\theta = 15°–90°$, using the 0.154 nm of Cu kα radiation source. X-ray photoelectron spectroscopy was taken on an XSAM800 XPS system with a Cu Kα source. Morphology of the thin films was observed using an atomic force microscope (AFM, SPI-300HV) with the scanning range of 1000 nm × 1000 nm under the scan pattern of noncontact.

2.3. Antibacterial Test. The antibacterial test was carried out in the aseptic room throughout the experiment. The antibacterial activity of the Fe-doped TiO_2 films and bare TiO_2 films was evaluated by the method of GB/T 5750.12–2006 [39]. The strain of *Escherichia coli* (*E. coli* ATCC 8739) was cultured in the solid medium and liquid medium, respectively. The lactose peptone suitable for *E. coli* growth was used to configure liquid medium and agar for medium configuration. Firstly, the bacteria were prepared using nutrient agar [39] and cultured in an incubator at 37 ± 1°C for 24 h, and then the prepared bacteria were transferred to a tube with a sloping solid medium and cultured again. After this, a small amount of bacteria were placed in a conical flask containing liquid medium followed by 24 h of culture. The initial concentration of bacterial solution was approximately 1×10^7 CFU/mL, and the concentration of experimental bacterial solution was achieved by dilution of 10 times with sterilized distilled water by a series of dilution methods.

A photocatalytic reactor used in the antibacterial test is shown in Figure 1, in which a 500 W xenon lamp (it mainly provides visible light in the range of 400–700 nm) used to simulate the solar light was positioned inside the reactor surrounded by a circulating water jacket to cool the reaction temperature. Four films were placed vertically on a shelf in a covered beaker which is inoculated with 500 ml of 10^5 CFU/ml of bacteria. At the other side of the reactor, the reference with 4 bare TiO_2 films was configured in the same way. The sample and reference were parallel to the light source. The magnetic stirrer was used to ensure that the solution is mixed evenly throughout the experiment. The antibacterial rate of bacteria of the TiO_2 films can be calculated by following formula:

$$R = \frac{(c - a)}{c} \times 100\%, \tag{1}$$

where R is the antibacterial rate, %; c is the colony count of reference samples, CFU/ml, and the method of colony count is shown in supporting information: experimental section; and a is the colony count of TiO_2 films, CFU/ml.

3. Results and Discussion

The peak patterns of Raman spectra show that all the Fe-doped films exhibit five anatase Raman peaks around 144, 196, 397, 517, and 639 cm^{-1} which can be attributed to Ti-O vibrations [6, 40] (Figure 2). There was no peak due to iron oxide even for the heavily doped sample with 2.0 at% of Fe. Moreover, the intensity of characteristic peaks of Fe-doped TiO_2 tends to decrease gradually as the amount of the Fe dopant increases because Fe doping leads to lattice distortion and change in the crystallite size (Table 1) [41].

The XRD patterns (Figure 3) exhibit expected diffraction peaks at 25°, 38°, 48°, 53°, 55°, 62°, and 75° indexed as the (101), (004), (200), (105), (211), (204), and (215) crystalline plane of anatase TiO_2, respectively (JCPDS file no. 21–1272 [11]). Raman and XRD spectra show that no peaks of iron oxide were observed. Hence, the iron in the Fe-doped TiO_2 films should be highly dispersed in the titanium dioxide lattice.

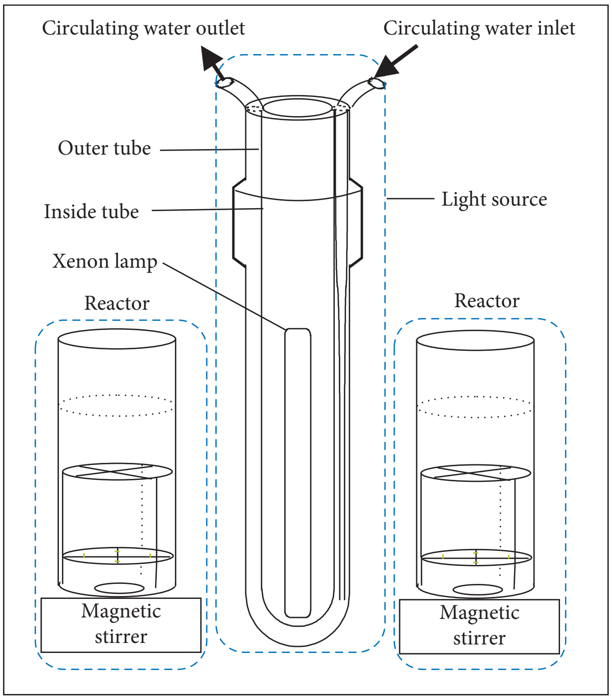

Figure 1: Photocatalytic reaction device for antibacterial experiment.

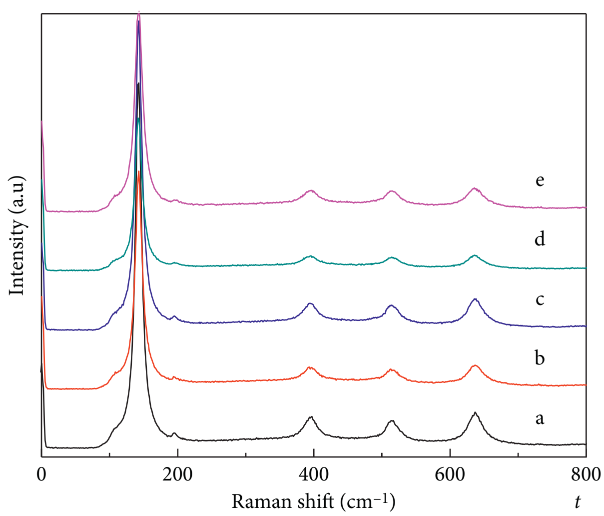

Figure 2: Raman spectra of (a) bare TiO_2, (b) 0.1 at%, (c) 0.5 at%, (d) 1.0 at%, and (e) 2.0 at% of Fe-doped TiO_2.

Table 1: Crystallite size and roughness of TiO_2 films with different atomic ratios of Fe to Ti.

No.	a	b	c	d	e
Fe content (at%)	0	0.1	0.5	1.0	2.0
Crystal size (nm)	21.53	19.24	19.58	21.03	22.24
RMS (nm)[a]	2.1	3.6	3.7	4.6	5.0

[a]RMS, average roughness of TiO_2 was determined by AFM.

The XPS pattern of 1.0 at% of Fe-doped TiO_2 film shows that the peak of Fe 2p can be fitted into two peaks at binding energies of 723.8 and 711.1 eV, which are attributed to Fe

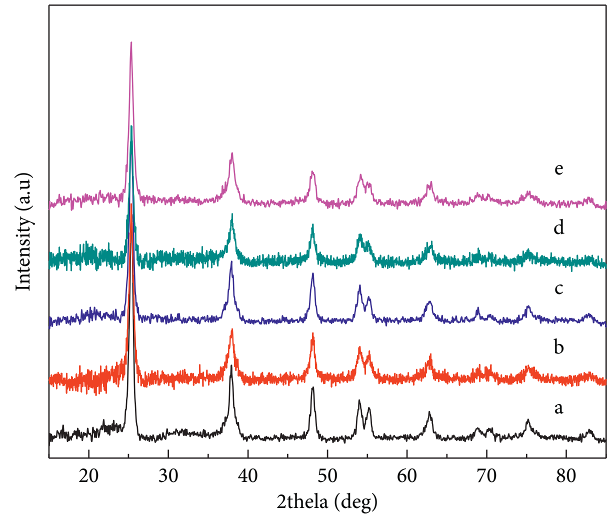

Figure 3: X-ray diffraction patterns of (a) bare TiO_2, (b) 0.1 at%, (c) 0.5 at%, (d) 1.0 at%, and (e) 2.0 at% of Fe-doped TiO_2.

$2p_{1/2}$ and Fe $2p_{3/2}$, respectively, and the two peaks correspond to those of Fe^{3+} (Figure 4).

AFM imaging was used to observe the surface morphology of the samples. It was observed that the films are composed of nanocrystalline islands of different sizes. For bare TiO_2 films, it forms scattered ellipsoidal nanoparticles of various sizes on the glass substrate, with an average particle size around 42 nm (Figure S3). After Fe-doping, the thin and dense needle-like nanoparticles appeared on the surface of the films with more deep valley formation by voids and peaks formation by protrusions between the nanoparticles (Figure 5). In our experiments, the nanocrystalline particles on the surface of the film are connected into flakes in the atomic ratio of Fe : Ti = 2.0 at%, resulting in massive deep valleys and obvious peaks (Figure S4). This confirms that the crystal size of TiO_2 is changed and indicates changes in the roughness of the samples. The roughness data are in good agreement with this prediction, with increasing roughness for Fe-doped TiO_2 films (Table 1).

The effect of obtained Fe-doped TiO_2 films on the antibacterial activity of *E. coli* was determined by evaluation of the growth of the cultures under irradiation from a xenon lamp source, compared with the growth of the bacterial cultured in TiO_2 film only. Figure 6(a) showed the agar plate was covered with bacterial colonies before illumination. After 3 h of photocatalytic reaction, 0.1% of Fe-doped TiO_2 film was much better to prevent the growth of colonies of *E. coli* as can be seen in Figure 6(c), compared with the bare TiO_2 film (Figure 6(d)) which showed limited antibacterial property.

To determine the appropriate amount of Fe doping, samples containing 0, 0.1, 0.5, 1.0, 2.0, and 3.45 at% of Fe-doped TiO_2 films were used in antibacterial testing. Figure 7 shows the antibacterial rate at each time point for both reference and test samples. After one hour of the experiment, 0.1, 0.5, and 1.0 at% of Fe-doped TiO_2 films showed much higher antibacterial rate than that of the bare TiO_2 film, and it has reached more than 60% in 0.1% of Fe-doped TiO_2 film.

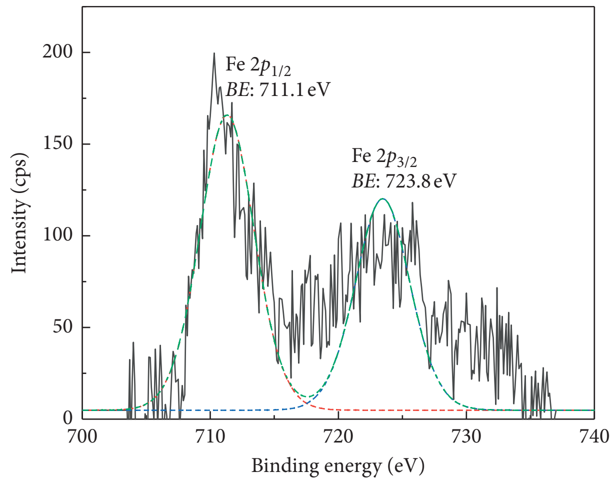

FIGURE 4: XPS spectrum of the Fe 2p peak of 1.0 at% of Fe-doped TiO_2 film.

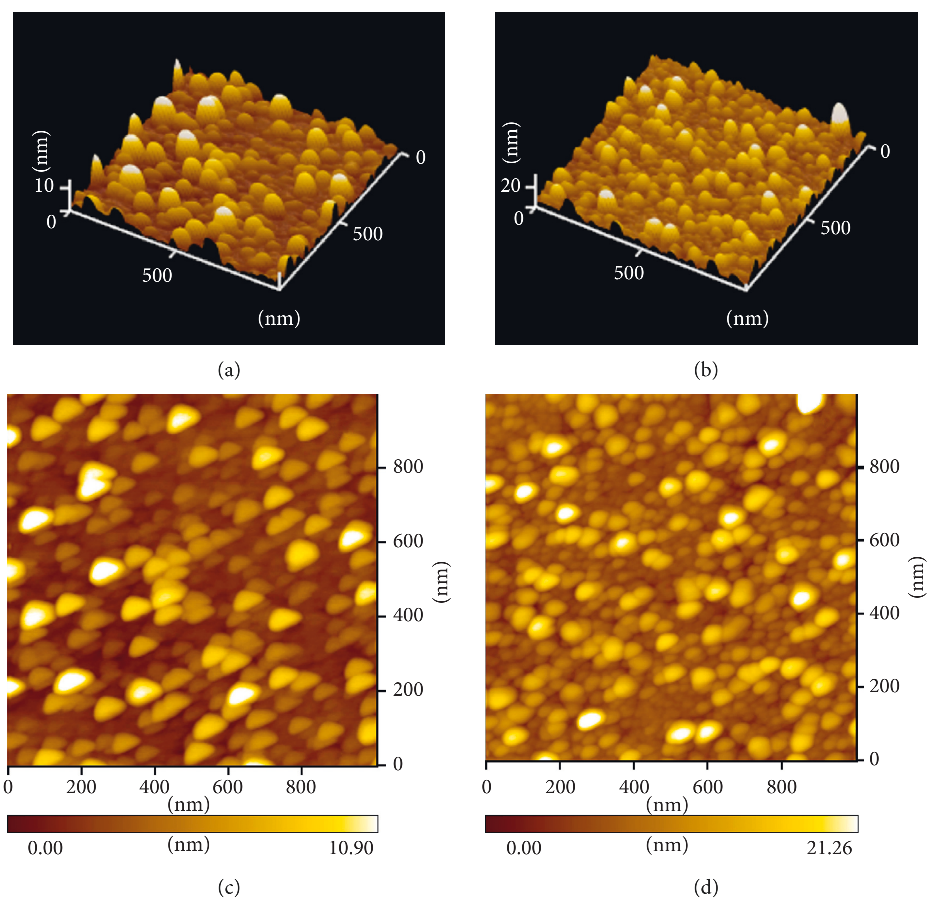

FIGURE 5: 3D AFM images of (a) bare TiO_2 films and (b) 0.1 at% of Fe-doped TiO_2 films; 2D AFM images of (c) TiO_2 films and (d) 0.1 at% of Fe-doped TiO_2 films.

At the end of the experiment, the antibacterial rate of TiO_2 films with doping ratio of less than 2.0 at% was much higher than that of bare TiO_2 film and it decreased with the increase of Fe dopant ratio above 2.0 at%. The order of antibacterial activity of TiO_2 films was as follows: 0.1 at% Fe > 0.5 at% Fe > 1.0 at% TiO_2 > bare TiO_2 > 2.0 at% Fe > 3.45 at% Fe-doping TiO_2. 0.1 at% of Fe is the optimum dopant ratio.

The antibacterial effect of obtained films was further investigated on the total bacteria in the real dye waste water. Dye waste water has the characteristics of large quantity, large alkalinity, deep chroma, and high content of organic pollutants, so it is still very difficult to deal with. Also, it contains a large number of microorganisms, including bacteria and fungi. 0.1 at% of Fe-doped TiO_2

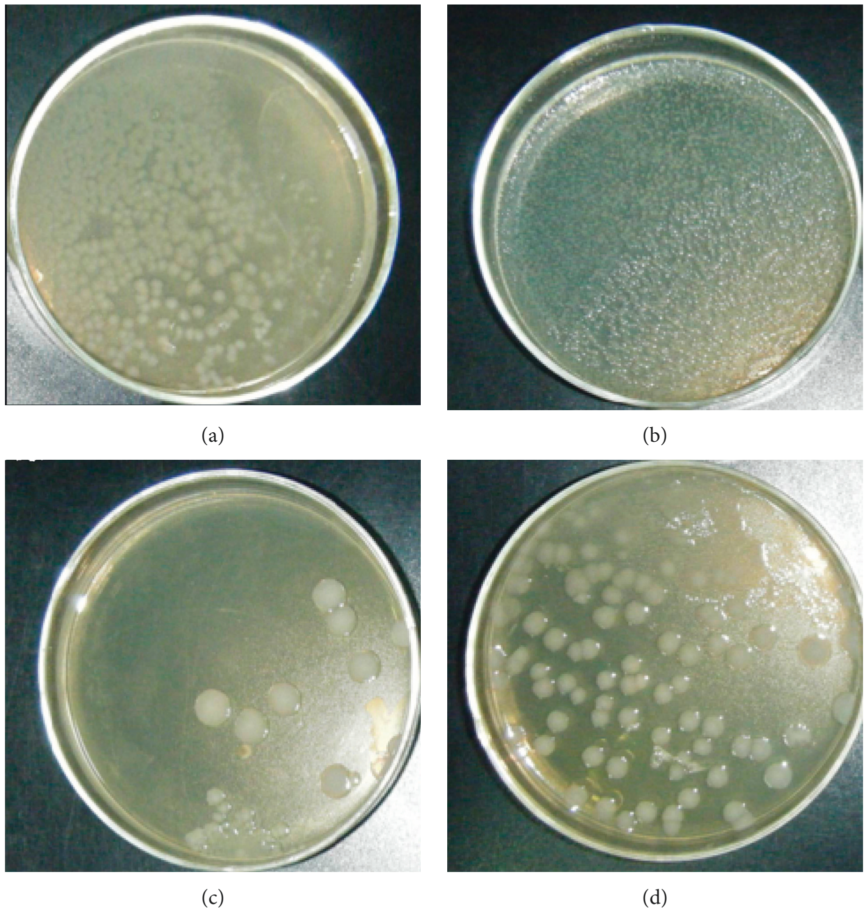

Figure 6: Agar plates before photocatalytic reaction (a) 0.1 at% of Fe-doped TiO_2 and (b) bare TiO_2, and after 3 h of photocatalytic reaction (c) 0.1 at% of Fe-doped TiO_2 and (d) bare TiO_2.

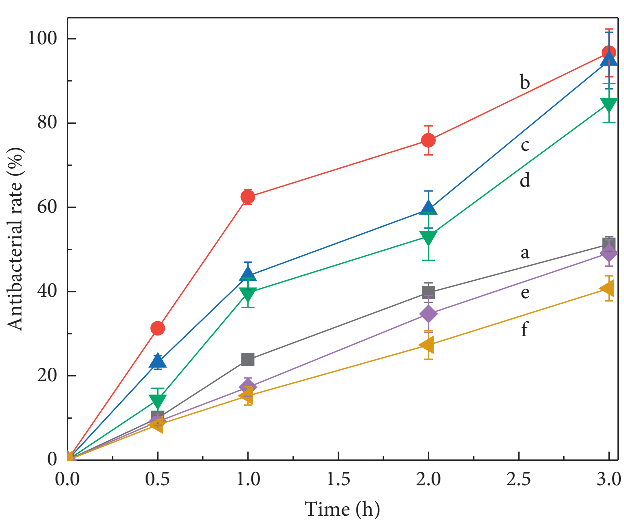

Figure 7: Antibacterial rate of (a) bare TiO_2, (b) 0.1 at%, (c) 0.5 at%, (d) 1.0 at%, (e) 2.0 at%, and (f) 3.45 at% of Fe-doped TiO_2 against *E. coli*.

film was selected to carry out this experiment by the same method as that of *E. coli* above. The dye waste water collected from a printing and dyeing factory was left for 24 h. The total bacteria in the supernatant were cultured and counted. It was then diluted to 1×10^5 CFU/mL for subsequent experimental measurements. The antibacterial properties of the film were tested under the illumination of a xenon lamp in the sterile room. The antibacterial rate of 0.1 at% of Fe-doped TiO_2 films was up to 97.57%, which is much higher than that of the bare TiO_2 film (Figure 8). This test showed that the Fe-doped TiO_2 films still have good antibacterial activity in a complex and real waste water, such as the coexistence of many bacteria and the presence of a large amount of organic compounds.

The modified TiO_2 nanomaterials such as Fe, Co, and V are reported that it can extend the spectral response of TiO_2 to the visible region [2, 10, 17, 42–46]. When the absorption range of TiO_2 is induced to the visible light region, the photocatalytic reaction occurs under the irradiation of solar light. The reaction involves the production of photogenerated holes and photoexcited electrons. These photogenerated holes can react with water to produce $^{\bullet}OH$ on the surface of the photocatalyst, and the photoexcited electrons can reduce oxygen to produce $O_2^{\bullet-}$ which can be further oxidized by photogenerated holes to form O_2. Then, the photogenerated holes can continue to react to produce other

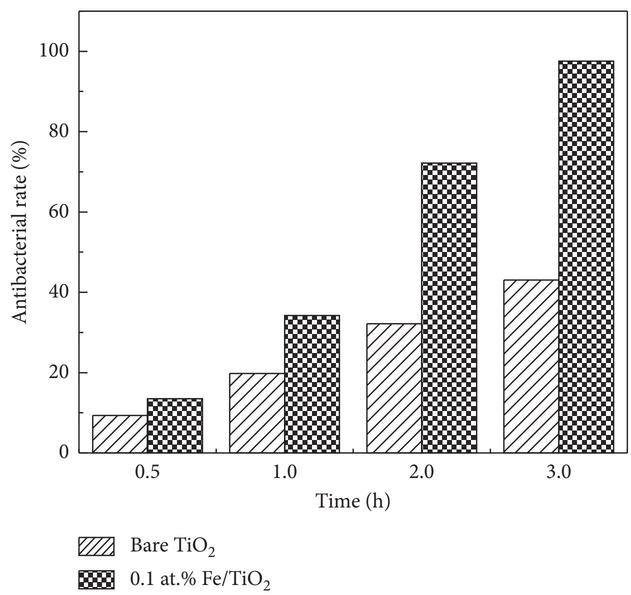

FIGURE 8: Antibacterial rate of 0.1 at% of Fe-doped TiO_2 film and bare TiO_2 film in dye waste water.

highly oxidizing species such as H_2O_2 or $^{\bullet}OOH$. These reactive oxygen species are toxic to the bacteria. They are in contact with bacteria on the surface of the obtained films and can degrade the cell of the bacteria by oxidizing the cell membrane, leading to loss of bacterial cell components and cell death. However, photocatalytic activity depends on the amount of doping agent. Excessive doping of metal will remain on the surface of the films and block reaction sites, resulting in a decrease in the activity of photocatalytic reaction [47]. Just as in our experiment, more than 2.0 at% of the Fe-doping TiO_2 film shows a decrease in antibacterial activity.

4. Conclusion

Antibacterial properties of the TiO_2 films under visible light with different molar ratios of Fe to Ti prepared by a sol-gel dip-coating method were studied and compared with the bare TiO_2 film. The Fe-doped TiO_2 films are mainly in the form of Fe^{3+}. When the doping concentration is more than 2.0 at%, the antibacterial properties of the Fe-doped TiO_2 films was lower than that of the bare TiO_2 films. Low level of Fe doping less than 2.0 at% showed excellent antibacterial activity even in real dye waste water.

Data Availability

The data used to support the findings of this study are included within the article and supplementary information file.

Conflicts of Interest

The authors declare that they have no conflicts of interest.

Authors' Contributions

C. X. designed the study. D. M. performed most of the reactions. X. L. performed some bacterial activity tests. Y. X., Y. Y., and Y. D. performed some characterization and analysis. D. M. and C. X. wrote the paper.

Acknowledgments

This work was supported by INPC Innovation Funds (grant no. 2014CX03).

Supplementary Materials

Figure S1: thickness of TiO_2 films with films with different coating layers. Figure S2: X-ray diffraction patterns of 2 at% of Fe-doped TiO_2 at different calcined temperatures. Figure S3: statistical results of particle size in a bare TiO_2 film (a) and 0.1 at% Fe-doped TiO_2 films (b). Figure S4: 3D AFM images of TiO_2 films with different Fe-doping amounts. Experimental section: colony counting method. (*Supplementary Materials*)

References

[1] J. A. Byrne, P. A. Fernandez-Ibañez, P. S. M. Dunlop, D. M. A. Alrousan, and J. W. J. Hamilton, "Photocatalytic enhancement for solar disinfection of water: a review," *International Journal of Photoenergy*, vol. 2011, Article ID 798051, 12 pages, 2011.

[2] M. Pelaez, N. T. Nolan, S. C. Pillai et al., "A review on the visible light active titanium dioxide photocatalysts for environmental applications," *Applied Catalysis B: Environmental*, vol. 125, pp. 331–349, 2012.

[3] S. Malato, P. Fernández-Ibáñez, M. I. Maldonado, J. Blanco, and W. Gernjak, "Decontamination and disinfection of water by solar photocatalysis: recent overview and trends," *Catalysis Today*, vol. 147, no. 1, pp. 1–59, 2009.

[4] D. W. Synnott, M. K. Seery, S. J. Hinder, G. Michlits, and S. C. Pillai, "Anti-bacterial activity of indoor-light activated photocatalysts," *Applied Catalysis B: Environmental*, vol. 130-131, pp. 106–111, 2013.

[5] P. S. M. Dunlop, M. Ciavola, L. Rizzo, and J. A. Byrne, "Inactivation and injury assessment of Escherichia coli during solar and photocatalytic disinfection in LDPE bags," *Chemosphere*, vol. 85, no. 7, pp. 1160–1166, 2011.

[6] J. Podporska-Carroll, E. Panaitescu, B. Quilty, L. Wang, L. Menon, and S. C. Pillai, "Antimicrobial properties of highly efficient photocatalytic TiO_2 nanotubes," *Applied Catalysis B: Environmental*, vol. 176-177, pp. 70–75, 2015.

[7] P. K. J. Robertson, J. M. C. Robertson, and D. W. Bahnemann, "Removal of microorganisms and their chemical metabolites from water using semiconductor photocatalysis," *Journal of Hazardous Materials*, vol. 211-212, pp. 161–171, 2012.

[8] R. Fagan, D. E. McCormack, D. D. Dionysiou, and S. C. Pillai, "A review of solar and visible light active TiO_2 photocatalysis for treating bacteria, cyanotoxins and contaminants of emerging concern," *Materials Science in Semiconductor Processing*, vol. 42, pp. 2–14, 2016.

[9] X. Z. Li and F. B. Li, "Study of $Au/Au^{3+}-TiO_2$ Photocatalysts toward visible photooxidation for water and wastewater treatment," *Environmental Science & Technology*, vol. 35, no. 11, pp. 2381–2387, 2001.

[10] C. Y. W. Lin, D. Channei, P. Koshy, A. Nakaruk, and C. C. Sorrell, "Effect of Fe doping on TiO_2 films prepared by spin coating," *Ceramics International*, vol. 38, no. 5, pp. 3943–3946, 2012.

[11] S. M. H. AL-Jawad, A. A. Taha, and M. M. Salim, "Synthesis and characterization of pure and Fe doped TiO_2 thin films for antimicrobial activity," *Optik*, vol. 142, pp. 42–53, 2017.

[12] A. Fujishima, K. Hashimoto, and T. Watanabe, *TiO_2 Photocatalysis: Fundamentals and Applications*, BKC Inc., Tokyo, Japan, 1999.

[13] D. A. Keane, K. G. McGuigan, P. F. Ibáñez et al., "Solar photocatalysis for water disinfection: materials and reactor design," *Catalysis Science & Technology*, vol. 4, no. 5, pp. 1211–1226, 2014.

[14] H. M. Yadav, S. V. Otari, V. B. Koli et al., "Preparation and characterization of copper-doped anatase TiO_2 nanoparticles with visible light photocatalytic antibacterial activity," *Journal of Photochemistry and Photobiology A: Chemistry*, vol. 280, pp. 32–38, 2014.

[15] A. M. Czoska, S. Livraghi, M. Chiesa et al., "The nature of defects in fluorine-doped TiO_2," *The Journal of Physical Chemistry C*, vol. 112, no. 24, pp. 8951–8956, 2008.

[16] P. A. Charpentier, C. Chen, K. Azhie et al., "Photocatalytic and antibacterial activities of silver and iron doped titania nanoparticles in solution and polyaspartic coatings," *Nanotechnology*, vol. 30, no. 8, Article ID 085706, 2018.

[17] N. Murakami, A. Ono, M. Nakamura, T. Tsubota, and T. Ohno, "Development of a visible-light-responsive rutile rod by site-selective modification of iron (III) ion on {111} exposed crystal faces," *Applied Catalysis B: Environmental*, vol. 97, no. 1-2, pp. 115–119, 2010.

[18] J. A. Rengifo-Herrera, J. Kiwi, and C. Pulgarin, "N, S co-doped and N-doped Degussa P-25 powders with visible light response prepared by mechanical mixing of thiourea and urea. Reactivity towards E. coli inactivation and phenol oxidation," *Journal of Photochemistry and Photobiology A: Chemistry*, vol. 205, no. 2-3, pp. 109–115, 2009.

[19] J. A. Rengifo-Herrera and C. Pulgarin, "Photocatalytic activity of N, S co-doped and N-doped commercial anatase TiO_2 powders towards phenol oxidation and E. coli inactivation under simulated solar light irradiation," *Solar Energy*, vol. 84, no. 1, pp. 37–43, 2010.

[20] C. W. Dunnill, Z. Ansari, A. Kafizas et al., "Visible light photocatalysts-N-doped TiO_2 by sol-gel, enhanced with surface bound silver nanoparticle islands," *Journal of Materials Chemistry*, vol. 21, no. 32, Article ID 11854, 2011.

[21] J. C. Yu, W. Ho, J. Yu, H. Yip, P. K. Wong, and J. Zhao, "Efficient visible-light-induced photocatalytic disinfection on sulfur-doped nanocrystalline titania," *Environmental Science & Technology*, vol. 39, no. 4, pp. 1175–1179, 2005.

[22] A. A. Ashkarran, H. Hamidinezhad, H. Haddadi, and M. Mahmoudi, "Double-doped TiO_2 nanoparticles as an efficient visible-light-active photocatalyst and antibacterial agent under solar simulated light," *Applied Surface Science*, vol. 301, pp. 338–345, 2014.

[23] M. B. Fisher, D. A. Keane, P. Fernández-Ibáñez et al., "Nitrogen and copper doped solar light active TiO_2 photocatalysts for water decontamination," *Applied Catalysis B: Environmental*, vol. 130-131, pp. 8–13, 2013.

[24] M. C. Wang, H. J. Lin, and T. S. Yang, "Characteristics and optical properties of iron ion (Fe^{3+})-doped titanium oxide thin films prepared by a sol-gel spin coating," *Journal of Alloys and Compounds*, vol. 473, no. 1-2, pp. 394–400, 2009.

[25] G. H. Takaoka, T. Nose, and M. Kawashita, "Photocatalytic properties of Cr-doped TiO_2 films prepared by oxygen cluster ion beam assisted deposition," *Vacuum*, vol. 83, no. 3, pp. 679–682, 2008.

[26] C. Karunakaran, G. Abiramasundari, P. Gomathisankar, G. Manikandan, and V. Anandi, "Cu-doped TiO_2 nanoparticles for photocatalytic disinfection of bacteria under visible light," *Journal of Colloid and Interface Science*, vol. 352, no. 1, pp. 68–74, 2010.

[27] S. Mathew, P. Ganguly, S. Rhatigan et al., "Cu-doped TiO_2: visible light assisted photocatalytic antimicrobial activity," *Applied Sciences*, vol. 8, no. 11, p. 2067, 2018.

[28] L. Jing, B. Xin, F. Yuan, L. Xue, B. Wang, and H. Fu, "Effects of surface oxygen vacancies on photophysical and photochemical processes of Zn-doped TiO_2 Nanoparticles and their relationships," *The Journal of Physical Chemistry B*, vol. 110, no. 36, pp. 17860–17865, 2006.

[29] B. Cao, S. Cao, P. Dong, J. Gao, and J. Wang, "High antibacterial activity of ultrafine TiO_2/graphene sheets nanocomposites under visible light irradiation," *Materials Letters*, vol. 93, pp. 349–352, 2013.

[30] R. Akbarzadeh, M. Ghaedi, S. Nasiri Kokhdan et al., "Electrochemical hydrogen storage, photocatalytical and antibacterial activity of Fe Ag bimetallic nanoparticles supported on TiO_2 nanowires," *International Journal of Hydrogen Energy*, vol. 43, no. 39, pp. 18316–18329, 2018.

[31] S. Larumbe, M. Monge, and C. Gómez-Polo, "Comparative study of (N, Fe) doped TiO_2 photocatalysts," *Applied Surface Science*, vol. 327, pp. 490–497, 2015.

[32] D. I. Anwar and D. Mulyadi, "Synthesis of Fe-TiO_2 composite as a photocatalyst for degradation of methylene blue," *Procedia Chemistry*, vol. 17, pp. 49–54, 2015.

[33] H. Moradi, A. Eshaghi, S. R. Hosseini, and K. Ghani, "Fabrication of Fe-doped TiO_2 nanoparticles and investigation of photocatalytic decolorization of reactive red 198 under visible light irradiation," *Ultrasonics Sonochemistry*, vol. 32, pp. 314–319, 2016.

[34] U. Arellano, M. Asomoza, and F. Ramírez, "Antimicrobial activity of Fe-TiO_2 thin film photocatalysts," *Journal of Photochemistry and Photobiology A: Chemistry*, vol. 222, no. 1, pp. 159–165, 2011.

[35] H. Dadvar, G. Khayati, and F. E. Ghodsi, "Optical, surface morphological, and antibacterial properties of nanostructured TiO2: M (M = Fe, Ce, Ag) thin films," *International Journal of Multidisciplinary and Scientific Emerging Research*, vol. 3, no. 1, pp. 951–956, 2014.

[36] C. C. Trapalis, P. Keivanidis, G. Kordas et al., "TiO_2 (Fe^{3+}) nanostructured thin films with antibacterial properties," *Thin Solid Films*, vol. 433, no. 1-2, pp. 186–190, 2003.

[37] W. Sangchay, P. Chantawee, A. Namesai, and D. Nanomater, "Fe doped TiO_2 thin films coated on glass fiber to inhibit bacterial of E. Coli prepared by sol-gel method," *Digest Journal of Nanomaterials and Biostructures*, vol. 9, no. 4, pp. 1593–1601, 2014.

[38] S. Boonyod, W. Sutthisripok, and L. Sikong, "Antibacterial activity of TiO_2 and Fe^{3+} Doped TiO_2 Nanoparticles Synthesized at Low Temperature," *Advanced Materials Research*, vol. 214, pp. 197–201, 2011.

[39] Chinese Standards, *Standard Examination Methods for Drinking water-Microbiological Parameters, GB/T 5750*, China Standards Press, Beijing, China, 2006.

[40] R. Jaiswal, J. Bharambe, N. Patel, A. Dashora, D. C. Kothari, and A. Miotello, "Copper and nitrogen co-doped TiO_2 photocatalyst with enhanced optical absorption and catalytic activity," *Applied Catalysis B: Environmental,* vol. 168-169, pp. 333–341, 2015.

[41] M. F. Hossain, S. Biswas, T. Takahashi, Y. Kubota, and A. Fujishima, "Investigation of sputter-deposited TiO_2 thin

film for the fabrication of dye-sensitized solar cells," *Thin Solid Films*, vol. 516, no. 20, pp. 7149–7154, 2008.

[42] J. Zhu, F. Chen, J. Zhang, H. Chen, and M. Anpo, "$Fe_3 \pm TiO_2$ photocatalysts prepared by combining sol–gel method with hydrothermal treatment and their characterization," *Journal of Photochemistry and Photobiology A: Chemistry*, vol. 180, no. 1-2, pp. 196–204, 2006.

[43] W. Lin and Y. Lin, "Effect of vanadium (IV)-doping on the visible light-induced catalytic activity of titanium dioxide catalysts for methylene blue degradation," *Environmental Engineering Science*, vol. 29, pp. 447–452, 2012.

[44] S. Yadav and G. Jaiswar, "Review on undoped/doped TiO_2 nanomaterial; synthesis and photocatalytic and antimicrobial activity," *Journal of the Chinese Chemical Society*, vol. 64, no. 1, pp. 103–116, 2017.

[45] O. Frank, M. Zukalova, B. Laskova, J. Kürti, J. Koltai, and L. Kavan, "Raman spectra of titanium dioxide (anatase, rutile) with identified oxygen isotopes (16, 17, 18)," *Physical Chemistry Chemical Physics*, vol. 14, no. 42, pp. 14567–14572, 2012.

[46] N. Murakami, T. Chiyoya, T. Tsubota, and T. Ohno, "Switching redox site of photocatalytic reaction on titanium (IV) oxide particles modified with transition-metal ion controlled by irradiation wavelength," *Applied Catalysis A: General*, vol. 348, no. 1, pp. 148–152, 2008.

[47] M. Kang, "The superhydrophilicity of Al–TiO_2 nanometer sized material synthesized using a solvothermal method," *Materials Letters*, vol. 59, pp. 3122–3127, 2005.